Soft Matter

Solvent Structure Controlled SeedGel Formation Investigated using Miscible Binary Solvent

Journal:	*Soft Matter*
Manuscript ID	SM-ART-11-2024-001306.R1
Article Type:	Paper
Date Submitted by the Author:	29-Jan-2025
Complete List of Authors:	Xi, Yuyin; National Institute of Standards and Technology; University of Delaware, Department of Chemical & Biomolecular Engineering Li, Ruipeng; Brookhaven National Laboratory, Condensed Matter Physics and Materials Science Department Heller, William; Oak Ridge National Laboratory, Neutron Scattering Division Hong, Kunlun; Oak Ridge National Laboratory Chen, Wei-Ren; Oak Ridge National Laboratory, Zemborain, Aurora; The University of Chicago, Liu, Yun; National Institute of Standards and Technology,

Solvent Structure Controlled SeedGel Formation Investigated using Miscible Binary Solvent

Yuyin Xi [1,2*], Ruipeng Li [3], William T. Heller [4], Wei-Ren Chen [4], Kunlun Hong [5], Aurora A. Zemborain [6], Yun Liu [1,2,7**]

xiyuyin28@gmail.com; yunliu@udel.edu and yun.lliu@nist.gov

1. Center for Neutron Research, National Institute of Standards and Technology, Gaithersburg, MD, 20899, USA
2. Department of Chemical & Biomolecular Engineering, University of Delaware, Newark, DE, 19716, USA
3. National Synchrotron Light Source II, Brookhaven National Laboratory, Upton, NY 11973, USA
4. Neutron Scattering Division, Oak Ridge National Laboratory, Oak Ridge, TN 37831, USA
5. Center for Nanophase Materials Sciences, Oak Ridge National Laboratory, Oak Ridge, TN 37831, USA
6. Pritzker School of Molecular Engineering, University of Chicago, Chicago, IL 60637, USA
7. Department of Physics & Astronomy, University of Delaware, Newark, DE, 19716, USA

Abstract

Recently, solvent segregation driven gel (SeedGel) has been demonstrated to be a tunable and versatile way to stabilize bicontinuous structures in a binary solvent. Here, the structure properties of SeedGel prepared with miscible solvent, 3-methylpyridine (3MP)/water are systematically

investigated using ultra-small angle neutron scattering (USANS) and small angle X-ray and neutron scattering (SAXS and SANS, respectively). The structures of samples prepared with 3MP/water show similar behavior as one previous SeedGel prepared with lutidine/water. Interestingly, the deuteration of 3MP in this binary solvent significantly shifts the gelation temperature of SeedGel. The results also demonstrate that both components of the binary solvent can be exchanged between the formed two domains of a SeedGel when changing the sample temperature. Importantly, the binary solvent used for the SeedGel preparation does not need to have a bulk phase transition as a function of temperature. Our results show that the correlation length due to the density fluctuation of the binary solvent is about the same at the gelation transition temperature for all studied SeedGels prepared with different binary solvents. Thus, this correlation length seems to be a key controlling parameter for the SeedGel formation. It is noted that this observation not only holds in binary solvents that show a bulk phase separation but also exists in miscible binary solvents without bulk phase separation. The results here thus open a window to prepare SeedGels with a new set of binary solvents that may have been overlooked before and provide guidance for choosing appropriate miscible binary solvents that can be used to prepare SeedGels.

Introduction

In the past decades, bicontinuous structures have generated much attention across a wide range of research fields, including energy storage, catalysis, energy saving, memory devices, water treatment, and biomedical applications. [1–6] In the soft matter community, research related to bicontinuous structures spans various topics, including polymers, emulsions, and liquid crystals. [7–9] Their interesting mechanical properties and enhanced mass transport between liquid-filled

channels guaranteed a fertile ground for new materials to bloom. The formation of bicontinuous channels in a versatile and tunable manner is extremely important for designing advanced materials.

Since 2005, bicontinuous interfacially jammed emulsion gels (Bijels) have triggered wide-ranging research interest. [2,10–13] Bijels are composed of binary solvents that phase separate in response to temperature changes and particles that are neutrally wetted to both components of the binary solvents. The gel forms due to the jamming of particles at the liquid-liquid interface when the binary solvent is quenched into the two-phase region. During the phase separation of the binary liquids, the particles stay at the interface to arrest the bicontinuous structures. To prevent the macroscopic phase separation of the sample, a Bijel is often formed by fast quenching into the 2-phase region of the binary solvents. While Bijels are a very interesting class of gel systems, it is also well-known that the preparation of particle surface is nontrivial, which requires equal preference to both components of a binary solvent. To improve Bijels preparation methods, different approaches are explored to ease the stringent requirements for formation, including understanding the particle size effect,[14] implementing particles of different types,[12] changing the shape of particles such as rod-like particles, [15] and adding ion-pairing polymers. [11] The phase diagrams of the pure binary solvents are routinely used to guide researchers in selecting the right solvent system and temperature for Bijels formation. The solvent pairs of water/2,6-lutidine, [10] ethanediol-nitromethane, [13] ethylene carbonate/p-xylene, [12] and styrene trimer/ polybutene [16] have been studied. All those binary solvents phase separate by changing the temperature (partially miscible).

Recently, a different approach to forming bicontinuous structure gels using binary solvents was proposed and demonstrated and is named solvent segregation driven gel (SeedGel). [6,17–19] While

Bijel formation relies on the macroscopic phase separation of the binary solvents, SeedGel formation is triggered by the phase separation of the binary solvent on the nanometer scale before reaching the phase-separation temperature of the bulk solvents. The local phase separation drives the aggregation of nanoparticles. The formation of the gel by the particles, in turn, causes the macroscopic phase separation of the binary solvent commensurate with the bicontinuous channels formed by the particles. Instead of pinning at the interface between two phase-separated liquids as that in Bijel, the particles in SeedGel are closely packed within one of the solvent domains. The domains exhibit tortuous shapes with micrometer-sized channels. In the gel state, the structures of these bicontinuous channels remain the same despite the temperature change. However, the relative compositions of the two solvents in both domains keep changing due to the exchange of solvent molecules between domains.[18]

More interestingly, some SeedGels exhibit structural color, which opens a door to stimuli-responsive materials for controlling the light and heat flow. [18] By changing the temperature, the wavelength of the light passing through SeedGel can be reversibly adjusted due to the aforementioned solvent exchange between domains. For a given solvent system, temperature dictates the wavelength of light that transmits a SeedGel sample.

So far, structural tunability and reversibility of SeedGel have been extensively studied in a model binary solvent of water/2,6-lutidine.[6,17] The dynamics of particles in SeedGel were also investigated. It was found that the relaxation time in the SeedGel is closely related to the mechanical properties of the SeedGel. [19] As SeedGel is a complex system with a wide range of potential applications, exploring different binary solvent pairs is useful for developing a general design guideline for predicting new material selections. It can further extend the temperature

range of the gel formation, making it more versatile to accommodate the requirements of various applications.

In this work, we systematically investigate the structural properties of the SeedGel prepared with two binary solvents, 3-methylpyridine (3MP) /water and deuterated 3MP (d-3MP) /water. The optical properties of SeedGel using 3MP/water have been briefly mentioned in our prior publication. [18] However, the structure properties and the physical mechanisms of the gel formation were not investigated. In sharp contrast to the partially miscible binary solvents explored in many Bijel and SeedGel studies, there is no bulk macroscopic phase separation at ambient pressure at all temperatures for 3MP/water. [20–24] While the nanometer solvent phase separation is the key trigger to introduce the attraction between particles for SeedGel formation, all binary solvents used in most previously studied SeedGel systems have a macroscopic phase separation temperature of the bulk solvent not very far from the gel temperature. The formation of SeedGel in 3MP/water thus helps us further understand the role of a binary solvent in the SeedGel preparation. Here, we demonstrate that the correlation length due to the density fluctuation of a binary solvent seems to be a key controlling parameter for the SeedGel formation. This thus points to a new direction for discovering new binary solvents for SeedGel formation by working with binary solvents without macroscopic phase separation, which may have been overlooked before.

Experimental

Materials

Silica nanoparticle dispersion (Ludox TM-50, Lot # MKCG0820) was purchased from Sigma Aldrich (St Louis, MO). Hydrogenated solvents, h-3-methypyridine (h-3MP) and 2,6-lutidine, were ordered from Tokyo Chemical Industry (TCI, Portland, OR). Deuterated solvents, d-

3methylpyridine (d-3MP) and deuterium oxide, were obtained from Cambridge Isotope Laboratories (CIL, Tewksbury, MA). The chemicals were used as received without further purification. Distilled water was used in the preparation of the binary solvents.

SeedGel preparation

The preparation of SeedGel followed the previous work. [6,17–19] A brief summary is given here. 400 micro-liter of h-3MP (or d-3MP) was added to 1 milliliter of Ludox TM™ in a glass vial. It has been determined that the silica nanoparticles in Ludox TM™ are around 27 nm in diameter with 10 % size polydispersity.[6] Similar to SeedGel formed in 2,6-lutidine/H_2O, a gel forms as soon as 3MP is added to the silica nanoparticle dispersion. Repeated vortexing of the mixture in a capped vial ensured a well-mixed system. The vial was left overnight on a rolling mixer in ambient conditions, which applies a continuous slow shear to the sample. Eventually, a transparent and well-dispersed sample was formed. The SeedGel is induced upon increasing the temperature of the sample. Depending on the temperature, the formed SeedGel can be visibly opaque, which may become transparent by adjusting the temperature. The transparent sample also exhibits structural color under white light. The detailed characterizations and explanations of the optical properties are documented in our recent work.[18]

UV-vis spectroscopy

A Thermo Scientific Evolution 201 UV-VIS Spectrometer (Waltham, MA, US) was used to measure the temperature-dependent optical transmission spectrum. The samples were sealed in a cuvette with a path length of 1 mm. A Peltier element connected to a thermal bath was used to accurately control the temperature. A thermocouple was placed in the vicinity of the sample and

the temperature reading was recorded. For each temperature change, a sample was equilibrated for about 10 min before each measurement.

Small angle neutron scattering (SANS) and Ultra-small angle neutron scattering (USANS) measurements

SANS and USANS measurements on samples prepared in 3MP/H_2O system were conducted at the Spallation Neutron Source (SNS) at Oak Ridge National Laboratory (ORNL, Oak Ridge, TN). The SANS experiments were performed on the Extended Q-Range SANS Diffractometer (EQ-SANS, BL-6).[25] The scattering data were stitched together using 1-D profiles recorded at both 4 m and 8 m to achieve a q-range of 0.003 $Å^{-1} < q < 0.5$ $Å^{-1}$. Neutrons with a wavelength of 2.5 Å were selected for measurements at 4 m detector distance and 10 Å wavelength was used for measurements at 8 m detector distance. Banjo cells with 1 mm path-length were used. The scattering background from an empty Banjo cell was recorded and carefully subtracted. Peltier units circulated by an external thermal bath were used to control the temperature of each sample block between 20°C and 80°C. The USANS experiments were conducted on the BL-1A beamline at SNS,[25] which covers a q-range of 6×10^{-5} $Å^{-1} < q < 1 \times 10^{-3}$ $Å^{-1}$. The sample environment allowed the loading of 9 samples simultaneously. Each of the three blocks was able to independently control the temperature of 3 sample cells. Data reduction for SANS followed standard procedures implemented in drtsans.[26] Data reduction for USANS also followed standard procedures using the Python scripts developed for the instrument.

Part of the SANS experiments (Shown in the Supporting Information) was performed on the 30m NGB30 beamline at the NIST Center for Neutron Research (NCNR, Gaithersburg, MD, USA). [27] A q-range between 0.001 $Å^{-1}$ and 0.461 $Å^{-1}$, where q is the scattering wave vector, was obtained

by stitching data from three detector positions. The temperature was controlled with a precision of ± 0.1 ˚C using heating and cooling blocks driven by Peltier. More than 30 minutes is waited to ensure the equilibration of the sample after the temperature change. The scattering data collected at NIST was reduced using standard Igor (Wavemetrics, Portland, OR) macro. [28]

Small angle X-ray scattering (SAXS)

The SAXS experiments were conducted using 11-BM (complex materials scattering, CMS) beamline at the National Synchrotron Light Source II (NSLS-II) at the Brookhaven National Laboratory (BNL, Upton, NY). A 3-pole wiggler source was used for X-ray generation. A rectangular beam was defined by slits with a size of 0.2 mm H × 0.2 mm V. The samples were loaded into Boron-rich capillaries with an outside diameter of 1 mm (Charles Supper Company, Westborough, MA). The capillaries were sealed with epoxy. Multiple samples were loaded on a custom-designed heating stage for measurements at several temperatures from room temperature to 78 °C. The SAXS signals were collected by Pilatus 2M detector (Dectris) located in a distance of 5.05m. The distance was calibrated by Silver Behenate. The typical exposure time was 10s and there was a 10 min delay at each temperature to ensure equilibration of the sample.

Results and Discussion

Previously, solvent segregation driven gel (SeedGel) was demonstrated to be stabilized using nanoparticles in a phase-separating binary solvent. [6,17–19] To form a SeedGel, one of the solvent components has to preferentially wet the nanoparticle surface. A model binary solvent of 2,6-lutidine and water was used previously with a lower critical solution temperature (LCST) of 34

˚C. [6] As the gel formation is triggered by nanometer aggregates formation, this system forms SeedGel at about 26 °C, which is 8 °C below the temperature of the critical point of the bulk binary solvent. [6,17–19] The difference between the gelation temperature and the phase separation temperature of the binary solvent is because the SeedGel formation is triggered by the nanometer scale phase separation of the binary solvent, rather than macroscopic phase separation. In contrast, the widely studied bicontinuous interfacially jammed emulsion gel (Bijel) system requires a quench deep into the two-phase region to arrest the bicontinuous structure because macroscopic phase separation of the binary solvent is required in Bijel. [10,12,13] The regions of Bijel and SeedGel studied in the literature are schematically illustrated in Figure 1 (a). Bijel forms in the two-phase region of the binary solvent, where two components of a binary solvent macroscopically phase separate. In our previous work on SeedGel, we focused on a model system using water and 2,6-lutidine (partially miscible solvent with a macroscopic phase separation temperature). However, a miscible binary solvent, 3MP/water, has recently found to induce SeedGel formation as schematically illustrated in Figure 1 (b), which broadens the library of solvents that can be potentially used for SeedGel. Here, we systematically investigate the structures and properties of SeedGel prepared using h-3MP/water and d-3MP/water.

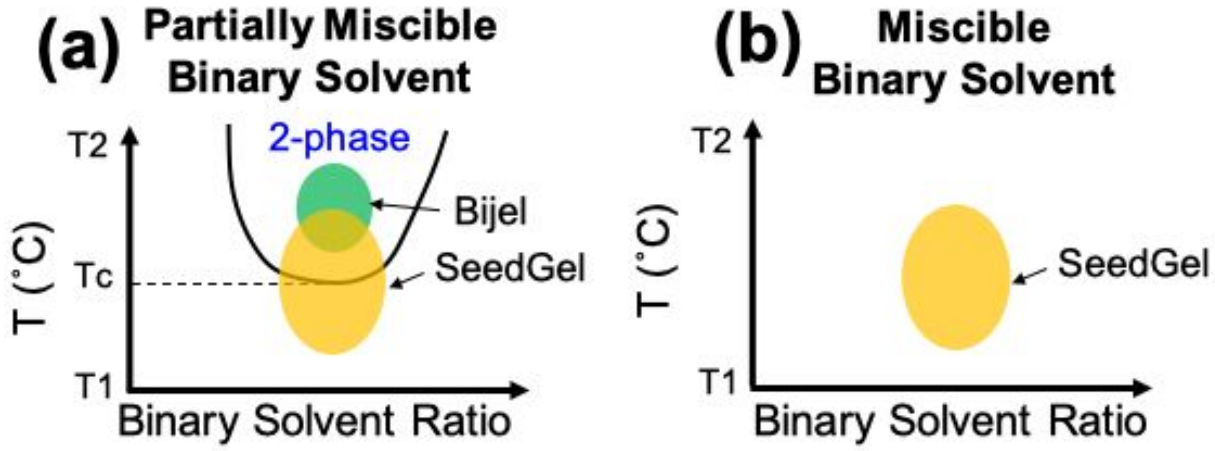

Figure 1. (a) Schematic phase diagram of both SeedGel and Bijel. SeedGel can be formed close to the critical temperature (T_c) of a binary solvent. Bijel is formed in the 2-phase region above the critical temperature. (b) Schematic drawing shows that SeedGel can also be formed in the binary solvent without T_c.

It is well documented that the binary mixture of 3MP and H_2O does not show a macroscopic phase separation at all concentrations at ambient pressure. [20–24,29] To verify this, optical transmissions are used to determine the phase separation temperature of this binary solvent as the transmitted intensity is expected to reduce near the phase separation temperature. [23] The decrease in light transmission is due to the strong scattering from the large droplets formed near the phase separation of binary solvents. UV-vis spectroscopy measurements in Figure S1 in the Supporting Information do not show any reduction in transmittance in h-3MP/H_2O between 20 ˚C and 90 ˚C. No visual sign of phase separation is observed within the same temperature range evidenced by the inset photographs of the binary solvent after heating up. Thus, our experiment also confirmed that the binary solvent sample of h-3MP/H_2O does not macroscopically phase separate at the temperature up to at least 90 °C at the ambient pressure.

Figure 2 (a) shows the USANS scattering profiles of the samples prepared with charged silica nanoparticles and hydrogenated 3-methylpyridine (h-3MP)/H_2O. The weak scattering intensity at 20 ˚C indicates that the sample is liquid with well-dispersed nanoparticles in the binary solvent and no micrometer-sized domains are observed in this q-range. The increase of the scattering intensity at 50 ˚C indicates the formation of micrometer particle domains and solvent channels, which are similar to the scattering features observed in SeedGel prepared using 2,6-lutidine/water. [6,17–19] A hump at $q \approx 1.3 \times 10^{-4}$ Å^{-1} suggests a well-repeated distance between domains. The scattering pattern can be modeled with the Teubner-Strey model, which is usually used to describe bicontinuous structures. [30–32] The fit results are plotted together with the experiment data in Figure 2(a). The details of the model are included in the Supporting Information. The periodicity of the structures is estimated to be around 5 μm (Table 1). By increasing the temperature to 70 ˚C, the q-position of the hump does not shift, except for a slight decrease in the intensity. This suggests that the size of the bicontinuous domains remains the same once the SeedGel forms. The intensity decrease is due to the solvent exchange between the bicontinuous domains, which alters the contrast between domains. (The solvent exchange will be discussed in detail later in this paper.) The scattering length densities (SLD) of silica, water (H_2O), and h-3MP are 3.47×10^{-6} Å^{-2}, -0.56×10^{-6} Å^{-2}, and 1.43×10^{-6} Å^{-2}, respectively. The solvent exchange causes the enrichment of water in the particle domain, which slightly reduces the averaged scattering length density (SLD) difference between the two domains. As the SLD of water and h-3MP are relatively close to each other, the scattering intensity due to the solvent exchange is small. Using the binary solvent of h-3MP/ H_2O greatly expands the temperature range in which the bicontinuous structures are stable. When prepared in 2,6-lutidine/ H_2O (a partially miscible solvent), the bicontinuous structures are stable within a relatively small temperature range, spanning only about 5 ˚C, from 27 ˚C to 32 ˚C.

[6,17] Outside this range, the domains of SeedGel prepared with 2,6-lutidine/ H_2O become unstable due to coarsening of the domains. In sharp contrast, SeedGel formed in hydrogenated 3MP (h-3MP) /H_2O does not show any discernible domain structure changes for over 20 ˚C (from about 50 ˚C to 70 ˚C). The much wider temperature range is attributed to the fact that there is no macroscopic phase separation in h-3MP/H_2O.

To probe the solvent exchange of binary solvent in the particle domain and solvent channel, deuterated 3-methylpyridine (d-3MP) is used in Figure 2 (b) to enhance the contrast between the two components of the binary solvent. The most discernible difference induced by using deuterated solvents is the dramatic change in the scattering intensity at different temperatures. It is attributed to the strong contrast change between the two bicontinuous domains resulting from solvent exchange. The SLD of d-3MP and H_2O is 5.8×10^{-6} Å^{-2} and -0.56×10^{-6} Å^{-2} respectively. Because of the dramatic SLD difference between H_2O and d-3MP, SANS/USANS patterns become very sensitive to any solvent exchange between particle domains and solvent channels. The particle and solvent volume fractions of the samples prepared with d-3MP are kept the same as those of hydrogenated 3MP (h-3MP) samples. The structure of the formed micrometer domains/channels at elevated temperatures of SeedGel prepared with d-3MP/ H_2O (Figure 2(b)) is similar to that of h-3MP/ H_2O.

The analysis of the USANS patterns reveals a domain periodicity of about 5 μm (Table 1), which is similar to those formed using h-3MP. The domain size of SeedGel using d-3MP/ H_2O is stable and the bicontinuous structures do not coarsen over a wide range of temperatures from 54 ˚C to 82 ˚C. The scattering intensity of SeedGel with d-3MP/H_2O increases with temperature, an opposite trend to that of the SeedGel prepared with h-3MP/H_2O. The SLD of the particle domain is higher than that of the solvent domain for samples prepared with h-3MP/H_2O. Increasing the temperature

of SeedGel in h-3MP/H_2O raises the water concentration in the particle domain, reducing its SLD. Consequently, the contrast between domains decreases with temperature in h-3MP/H_2O SeedGel. In the sample with d-3MP/ H_2O, the SLD of the particle domain is lower than that of the solvent domain because the SLD of d-3MP is much higher than that of h-3MP and silica. As the charged particles like water, heating the sample increases H_2O concentration in the particle domain, decreasing the particle domain's SLD further. Due to the mass balance, the enrichment of water in the particle domain results in the hiking of d-3MP concentration in the solvent channels, increasing the SLD of the solvent domain. Thus, raising the temperature increases the difference of SLD between domains, resulting in an intensity increase of one and a half orders of magnitude from 54 ˚C to 82 ˚C (Figure 2(b)). The reverse temperature dependence of the intensity change between the two types of samples prepared with h-3MP/H_2O and d-3MP/H_2O is thus due to the opposite change of the contrast (SLD difference) between domains. The solvent change induced scattering intensity change by using deuterated 3MP unambiguously proves the solvent exchange between the particle domain and the solvent channel. Combined with the contrast-variation experiment we performed in the system using H_2O/ D_2O mixture (contrast-matching) and 2,6-lutidine previously, [6] the results show that both components of the binary solvent exchange between two domains in response to temperature change.

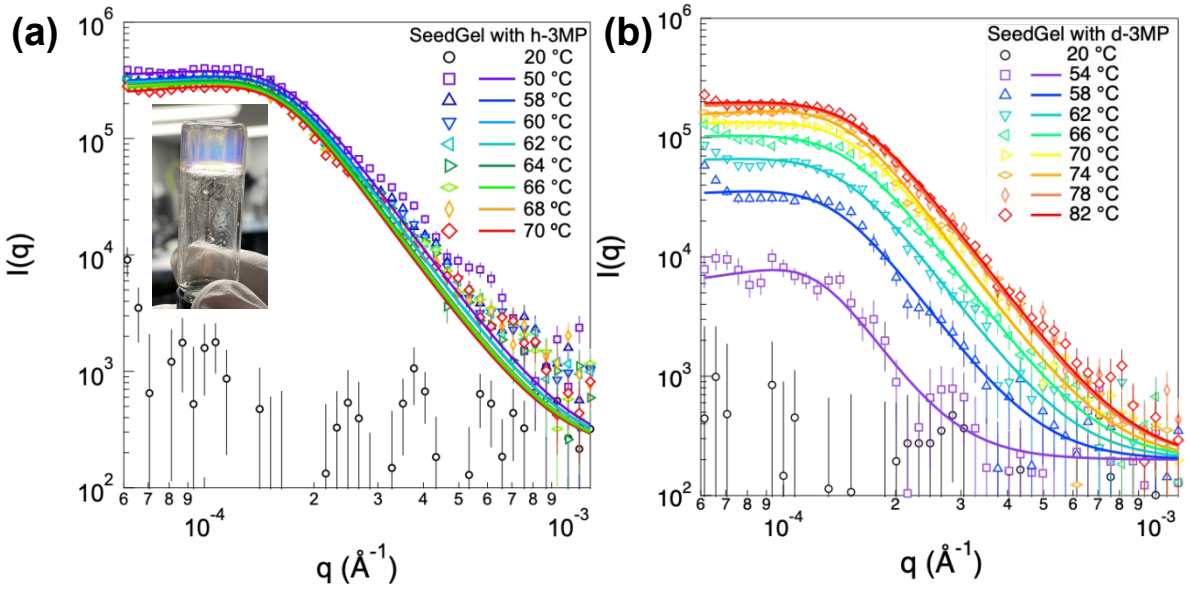

Figure 2. Smeared USANS profiles of SeedGel prepared with (a) hydrogenated and (b) deuterated 3-methylpyridine at different temperatures. The experimental data are plotted in open symbols and the fits based on the Teubner-Strey model are plotted in solid lines. The inset photo shows the formed gel in 3MP/H_2O, exhibiting structural colors. The error bars represent one standard deviation and are often smaller than the symbol size.

Table 1. The domain size and correlation length extrapolated from Teubner-Strey model fittings of SeedGel prepared in h-3MP/H_2O and d-3MP/H_2O.

h-3MP				**d-3MP**			
T (°C)	Domain size (μm)	Correlation Length (μm)	χ^2	T (°C)	Domain size (μm)	Correlation Length (μm)	χ^2
50	4.6 ± 0.03	1.1 ± 0.02	4.8	54	5.7 ± 0.2	1.8 ± 0.3	1.1

58	4.5 ± 0.04	1.1 ± 0.02	3.1	58	5.5 ± 0.1	1.3 ± 0.07	2.8
60	4.6 ± 0.03	1.1 ± 0.02	3.6	62	5.4 ± 0.08	1.2 ± 0.05	2.0
62	4.6 ± 0.03	1.1 ± 0.02	2.4	66	5.3 ± 0.07	1.1 ± 0.03	2.5
64	4.6 ± 0.03	1.2 ± 0.02	4.3	70	5.1 ± 0.05	1.1 ± 0.03	1.9
66	4.6 ± 0.03	1.2 ± 0.02	2.8	74	5.1 ± 0.04	1.2 ± 0.03	2.8
68	4.7 ± 0.03	1.1 ± 0.02	2.3	78	5.0 ± 0.04	1.1 ± 0.02	3.8
70	4.6 ± 0.03	1.1 ± 0.02	3.3	82	5.0 ± 0.05	1.0 ± 0.02	2.0

The dynamic solvent exchange between the particle domain and solvent domain in the gel state affects the temperature-dependent optical properties in some SeedGels,[18] as the wavelength of light passing through a sample is controlled by the temperature-dependent refractive index change of the bicontinuous domains. The refractive indexes of the two bicontinuous domains show different wavelength dependence (different dispersion curves). At a given temperature, the dispersion curves of the two domains only intersect at one wavelength. The refractive indexes mismatch at all other wavelengths. Light at the wavelength with a matched refractive index has the maximum transmission through the sample while others at different wavelengths are significantly attenuated. As the solvent exchanges between the bicontinuous domains with temperature, the refractive indexes of both domains change simultaneously. So does the wavelength of light with the maximum light transmission. This intriguing optical property is also observed with the h-3MP/H_2O. The photos in Figure 3(a) show the sample pictures during a

cooling process of a SeedGel prepared with h-3MP/H_2O. The color, due to the scattered light, changes from blue at higher temperatures to yellow. The transmittance during cooling is plotted against the wavelength in Figure 3(b) within the temperature range that shows color transition for SeedGel prepared in h-3MP/ H_2O. As indicated in the data, a peak transmittance is observed at one wavelength for the spectrum at each temperature. The light at the wavelength that are significantly attenduated is light scattering by the bicontinuous domains, which contributes to structural color. The yellow color (scattered color) appears when the refractive indexes of the two domains are matched at the short wavelength. Most blue light (short wavelength) is allowed to transmit through the sample, and the longer wavelengths (yellow) are scattered. Increasing the temperature allows the peak wavelength to shift to a longer wavelength, making the sample blue in color (short wavelengths are scattered). This explains the color transition in pictures in Figure 3(a) at different temperatures. To quantitatively compare the wavelength of the transmitted light at varying temperatures, the shortest wavelength that the sample first reaches 98 % of the peak transmittance (dashed line in Figure 3(b)) in a UV-vis measurement is plotted as a function of the temperature in Figure 3 (c). As the path length of the cuvette used is only 1 mm, the peak transmittance is broad at high temperatures. However, the peak of the transmitted light can be greatly sharpened by simply using a cuvette with a longer path length, as demonstrated previously.[18] For SeedGel prepared with h-3MP/H_2O, the temperature range with the adjustable optical transmission is between 40 ˚C and 50 ˚C. The onset temperature is also lower than that in d-3MP/ H_2O. By replacing h-3MP with its deuterated counterpart (d-3MP), the temperature of the visible light modulation is significantly increased by about 20 ˚C to approximately 60 ˚C. The working temperature change for SeedGel in d-3MP/H_2O is larger to achieve the same wavelength shift. In other words, the transmittance of SeedGel in h-3MP/H_2O is more sensitive to temperature

change. The isotope effect in SeedGel provides a general way to tune the temperature range of a SeedGel sample. Even though the isotope effect of water is well known to create an immiscible region in the phase diagram of 3MP/D_2O starting at around 40 ˚C, [24] we did not find a systematic study of the effect of 3MP deuteration on the phase diagram of the binary solvent of d-3MP/H_2O in the literature. Experimentally, we have determined that the binary solvent of d-3MP/H_2O does not show macroscopic phase separation within the temperature and concentration range of interest, evidenced by the identical optical transmission over a wide range of temperatures (Figure S2 in the Supporting Information). Thus, even though neither the binary solvent of h-3MP/H_2O nor d-3MP/H_2O shows macroscopic phase separation, they are still able to be used to prepare SeedGels. The SeedGels formed in this way also exhibit dynamically tunable optical transmission. The formation of SeedGel and its associated optical properties in a miscible binary solvent 3MP/H_2O indicates that SeedGel formation does not require the macroscopic phase separation temperature by the solvent themselves. This property expands the types of solvent systems that can be used for SeedGel formation. The results also demonstrate that isotopic substitution can be used to change the gelation/ color transition temperature of SeedGel without searching for new solvent pairs.

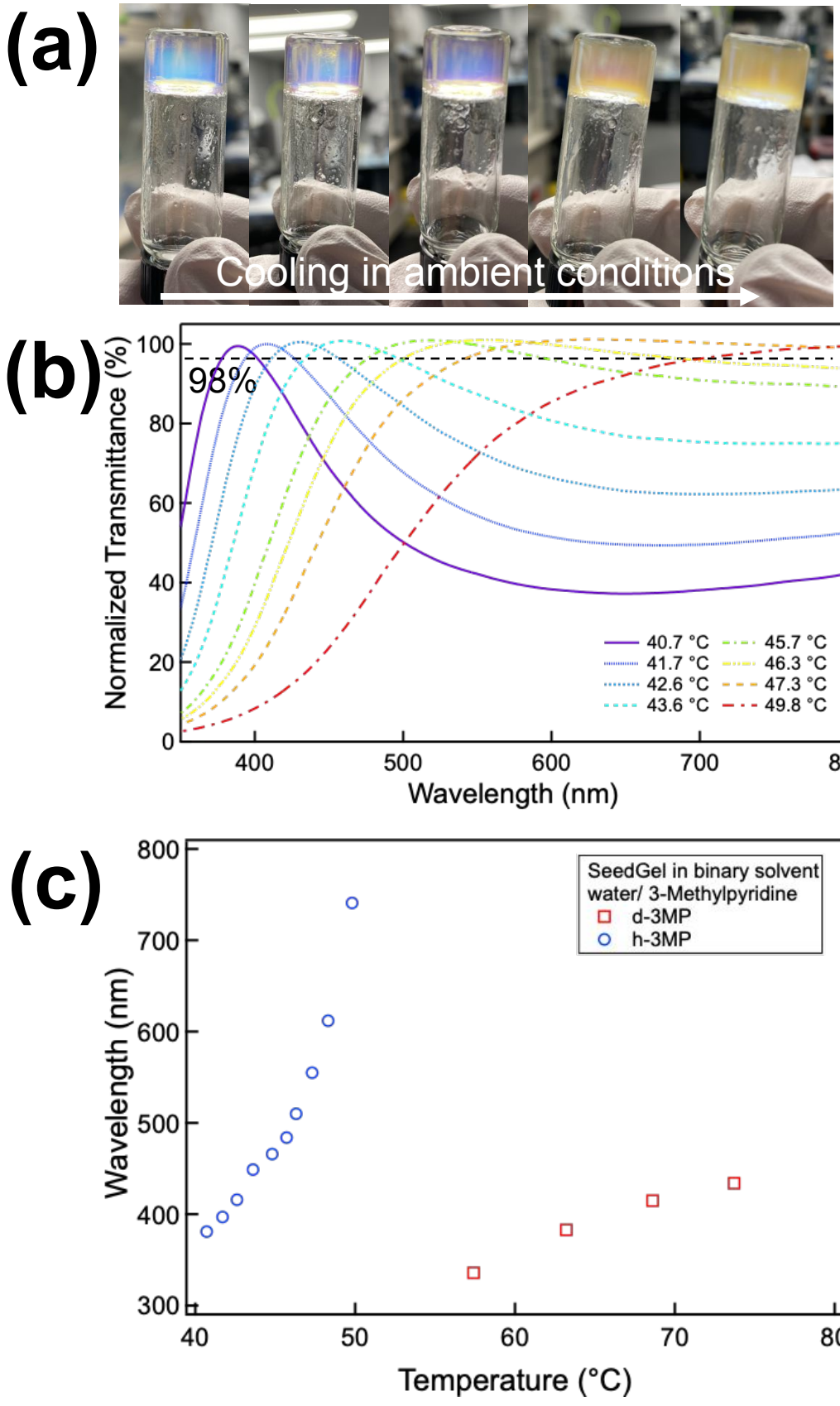
(a)
Cooling in ambient conditions
(b)
98%
Normalized Transmittance (%)
Wavelength (nm)
40.7 °C
41.7 °C
42.6 °C
43.6 °C
45.7 °C
46.3 °C
47.3 °C
49.8 °C
(c)
SeedGel in binary solvent
water/ 3-Methylpyridine
d-3MP
h-3MP
Wavelength (nm)
Temperature (°C)

Figure 3. (a) A series of photos of SeedGel prepared in h-3MP/H_2O taken during cooling at ambient conditions. (b) Normalized transmittance of SeedGel prepared in h-3MP/H_2O at different temperatures. The horizontal dashed line indicates 98 % of normalized transmittance. (c) The shorter wavelength that allows 98 % optical transmittance as a function of the measured temperature of SeedGel prepared with both deuterated and hydrogenated 3-methylpyridine. The volume fraction of 3-methylpyridine in the binary solvent is fixed at 36.4 % and the volume fraction of the silica nanoparticles is fixed at 22.7 % for both samples.

To investigate the structures at the nanometer scale during the SeedGel formation, small angle X-ray scattering (SAXS) experiments were performed on SeedGels at different temperatures (Figure 4). Figure 4 (a) shows the results of SeedGel in h-3MP/H_2O. The peak at around 0.023 $Å^{-1}$ is related to the average distance between silica nanoparticles. At temperatures below 36°C, silica nanoparticles are relatively uniformly dispersed in 3MP/H_2O. The SAXS pattern shows a broad hump at around 0.019 $Å^{-1}$, indicating that the sample is in the liquid state. Beginning at 36°C, the peak becomes sharper and gradually shifts to higher-q positions. This is due to the SeedGel formation with bicontinuous domains. The temperature increase drives the phase separation of the binary solvent at the surface of particles. At elevated temperatures, water is enriched on the particle surface, which attracts particles together to form aggregates due to capillary condensation. The random-sized aggregates explain the broad hump in the scattering profiles below 0.02 $Å^{-1}$ between 36°C and 40°C. As the sample is further heated, the water and particles aggregate together to minimize contact with 3MP. So, water becomes more and more enriched in the aggregates as temperatures increase. Eventually, bicontinuous particle domains percolate throughout the sample to form SeedGel, with water being the main solvent in the particle domain and the silica nanoparticles are tightly confined in the particle domain. The narrow distribution of the particle-particle distance results in a sharper peak in SAXS patterns, and a closer packing between particles leads to the peak shift to a high-q position, consistent with a previous study.[6] The peak position

shifts to around 0.0239 $Å^{-1}$ at temperatures above 40°C. The same trend is observed in SeedGel prepared in d-3MP/H_2O (Figure 4(b)), but with a drastically different transition temperature. The shift of the peak position to higher-q value does not occur until above 50°C, denoting a higher SeedGel formation temperature. The deuteration of one of the solvent components greatly increases the gelation temperature by more than 10 °C. The difference in SeedGel formation temperature is consistent with a much higher color transition temperature shown in Figure 3. Implementing d-3MP also exhibits a tighter particle packing when compared to SeedGel utilizing h-3MP. In the gel state, the q-position shifts to a higher-q value (0.0248 $Å^{-1}$), suggesting a reduced particle-particle distance for d-3MP SeedGel.

To better analyze the relationship between temperature and the structural change of SeedGel, the intensities at q = 0.003 $Å^{-1}$ and q = 0.1 $Å^{-1}$ are plotted as a function of temperature for SeedGel in Figure 4(c) and Figure 4(d), respectively. By raising the temperature from 25 °C, the initial intensity increase at low-q (below 0.01 $Å^{-1}$) before the SeedGel formation is due to the formation of the aggregates. A substantial change in the SAXS scattering profiles is observed during the gel formation. In Figure 4(c), the reduction of the intensity after reaching its maximum value is due to the formation of the micrometer bicontinuous domains, shifting the scattering profile to low-q value outside the q-range probed by SAXS. The difference in the transition temperature between the hydrogenated and the deuterated samples is about 10 °C based on the SAXS results, which is consistent with the UV-vis results shown in Figure 3. The intensity change at high-q (0.1 $Å^{-1}$) is also analyzed in Figure 4(d). The scattering intensity difference at this q-range is mainly related to the solvent composition change in the particle domain since it is mainly due to the change of the scattering length density difference between particles and solvent in the particle domain. By increasing the temperature, the intensities of both samples first increase slightly and then suddenly

decrease. The sharp decrease of the intensity at about 39 °C for 3MP/H_2O system indicates the solvent phase transition temperature. For the h-3MP/H_2O and d-3MP/H_2O systems, the transition temperature differs by about 10°C. For X-rays, the scattering length density (SLD) of H_2O is higher than that of 3MP. The SLD of silica is larger than both 3MP and water. A higher H_2O concentration near the particles results in a lower contrast between particles and the surrounding solvent, thus reducing the scattering intensity. Once the SeedGel forms, the scattering curves remain mostly unchanged as a function of temperature (Figure 4 (a) and Figure 4 (c)). Note that there are still small amounts of solvent exchanges between the particle domains and the fluid domains. Even though the exchange is large enough to change the optical properties, it is so small that its impact on the SAXS patterns is very minimal once the SeedGel forms. This is consistent with the USANS results (Figure 2(a) and Figure 2 (b)), where the high-q data are similar to each other at different temperatures above 50 °C in the gel state. In addition, the data around the high-q peak is fitted using the Hayter-Penfold method, from which the volume fraction of particles in the particle domain is estimated to be around 41 %. As the particles are tightly packed within the particle domain, the S(0) value is fairly small. The fitting results can be found in Figure S3 (a) and Figure S3 (b) in the supporting information. [33]

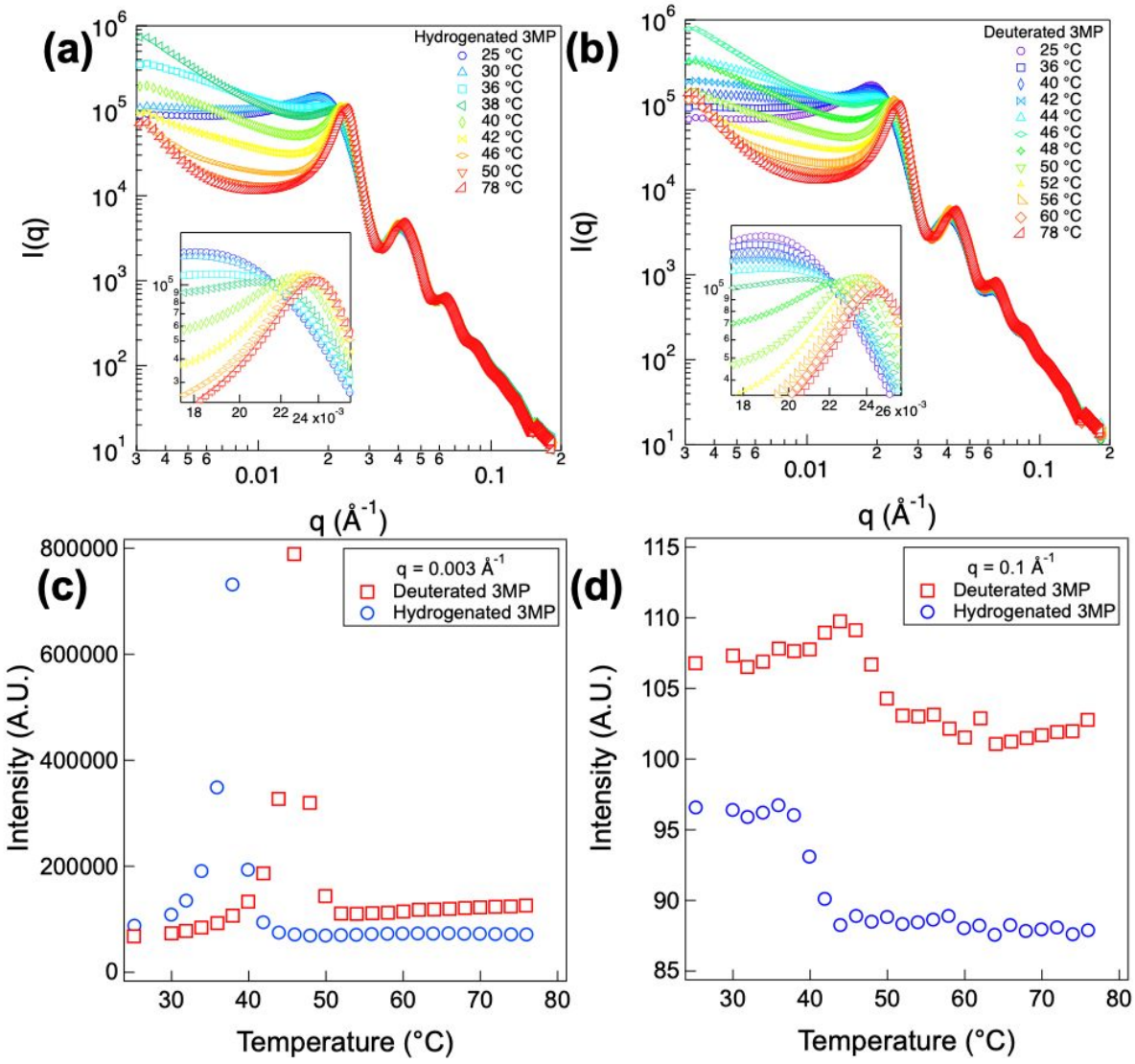

Figure 4. SAXS results of SeedGel prepared with (a) hydrogenated and (b) deuterated 3-methylpyridine measured at different temperatures. The comparison of the intensity between the two samples as a function of temperature at (c) 0.01 Å^{-1} and (d) 0.1 Å^{-1}.

To further understand the controlling factor of the binary solvent that drives the formation of SeedGel, small angle neutron scattering (SANS) measurements were used to study the properties of pure binary solvents for h-3MP/H_2O and d-3MP/H_2O at different temperatures. Despite h-3MP

and H_2O being fully miscible, SANS patterns show some structures at the nanometer scale with increasing temperature (Figure 5(a)). Similar SANS patterns are also observed for d-3MP/H_2O (Figure 5(b)). A Lorentz model is used to fit the scattering patterns of the binary solvent to obtain quantitative information. The details of the Lorentz model are shown in the Supporting Information. The fit results are plotted with the experimental data in Figure 5(a) and Figure 5(b).

The correlation length is obtained from the Lorentz model for binary solvents of both h-3MP/H_2O and d-3MP/H_2O. They are plotted as a function of temperature in Figure 5(c). In general, increasing the temperature increases the correlation length, indicating the formation of nanodomains of solvent molecules. For h-3MP/H_2O, the correlation length of the bulk solvent is about 20 Å at about 40 °C, which is the gelation transition temperature of the SeedGel prepared with h-3MP/H_2O. Interestingly, for the SeedGel prepared with d-3MP/H_2O, the correlation length of the bulk solvent for d-3MP/H_2O is also around 20 Å at the gelation temperature of the SeedGel, which is around 50 °C. Thus, for the same silica particle systems, it seems that the controlling factor of the SeedGel formation is the correlation length of bulk binary solvent. The correlation length of 2,6-lutidine and D_2O obtained from Lorentz model fitting is also studied and included in Figure 5(c). The SANS results of the binary solvents 2,6-lutidine/D_2O are plotted in Figure S4 in the Supporting Information. Note that in order to make a fair comparison between the SeedGels formed among the three systems, the same batch of silica nanoparticles was used. The vertical dashed lines in Figure 5(c) are the SeedGel gelation temperatures when prepared in the three binary solvents. Again, SeedGel forms when the correlation length of the binary solvent reaches around 20 Å. Therefore, this could be an important design guideline when choosing a binary solvent to prepare SeedGels from the silica particles used in this paper.

It has been previously observed that water-rich layers are adsorbed on the surface of charged silica nanoparticles. [34,35] The capillary condensation induced by solvent fluctuations acts as an attractive force to assemble nanoparticles in 2,6-lutidine/water mixture. [34,35] The formation of SeedGel is driven by this attractive force in the binary solvent. Even though no critical temperature exists in the mixtures of h-3MP/H_2O and d-3MP/H_2O for the temperature up to about 100 °C [23] , there is nanometer structure formation in 3MP/H_2O. The density fluctuation of around 2 nanometers would be enough to induce the formation of SeedGel. This critical correlation length is hypothesized to be related to the particle surface property and size. The correlation length is linked to the water absorption thickness, which is determined by the surface property of the nanoparticles. Due to the aforementioned attractive force, the absorbed liquid layer bridges the particles together to form aggregates. As a result, the further phase separation of the binary solvents is facilitated by the pores formed by the surrounding nanoparticles. The size of the pore, which is determined by the size of the nanoparticles, is closely related to the phase-separation of the solvents, thus, the formation of the SeedGel. It is hypothesized that the gelation temperature of SeedGel can be tuned by either the surface property or the particle size, which needs systematic investigations in the future.

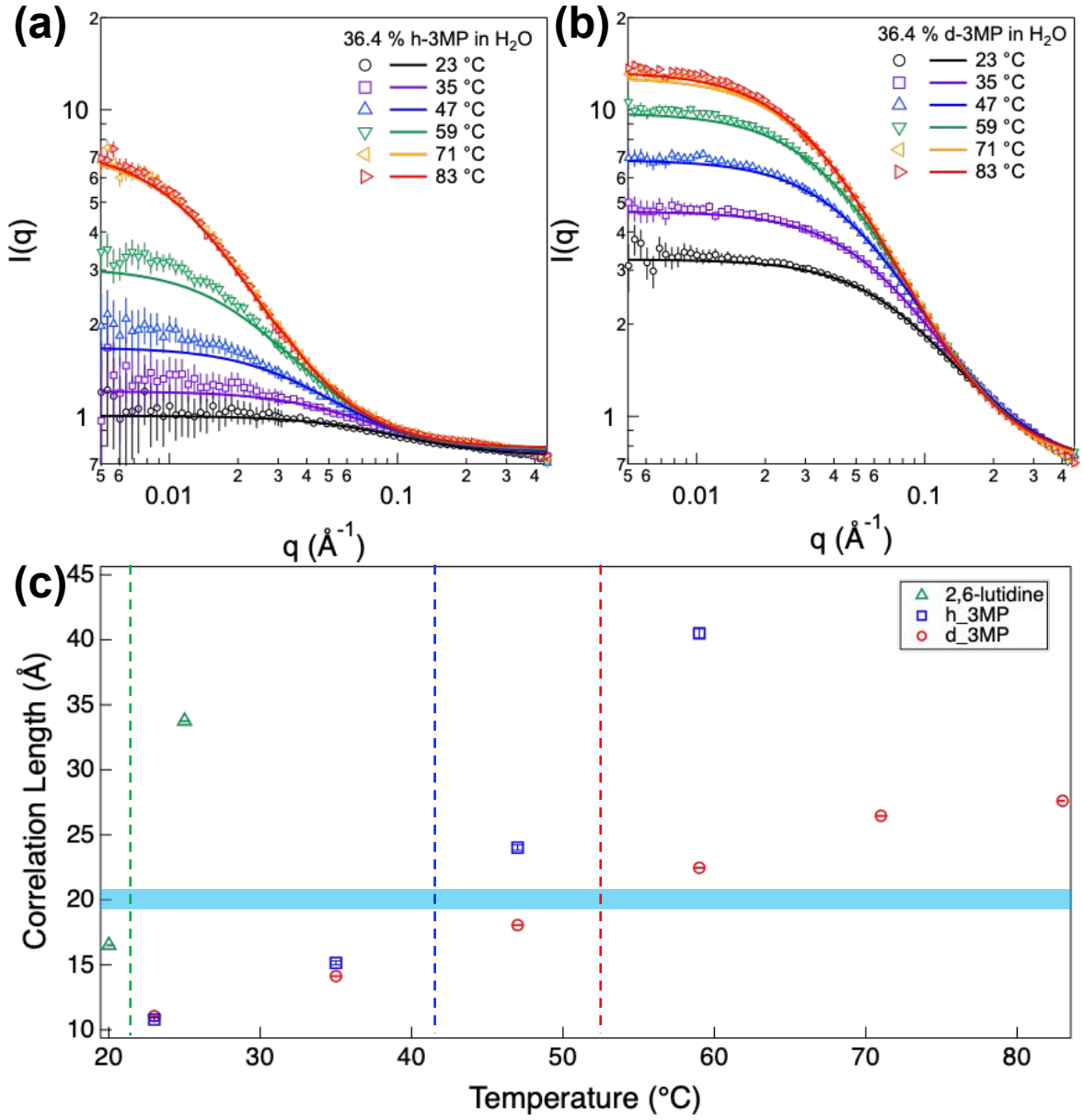

Figure 5. SANS profiles of the binary solvent of (a) hydrogenated 3-methylpyridine/ H_2O and (b) deuterated 3-methylpyridine/ H_2O at different temperatures. (c) The correlation length of 2.6-lutidine/D2O, h-3MP/H_2O, and d-3MP/H_2O, extrapolated from the Lorentz model at different temperatures. The green, blue, and red dashed lines represent the gelation temperatures of SeedGel prepared in the binary solvent of 2,6-lutidine/H_2O, h-3MP/H_2O, and d-3MP/H_2O, respectively. The blue stripe represents a general guideline that connects the critical correlation length in the three binary solvents together.

Conclusions

The microscopic structures of SeedGel prepared with h-3MP/H_2O and d-3MP/H_2O are systematically investigated here. Different from all the previous binary solvents used for the preparation of the SeedGel, the binary solvents studied in this paper do not show phase separation macroscopically for temperatures up to about 100 °C. Yet, nanoparticles dispersed in these two binary solvents can also form SeedGel. This distinguishes SeedGel from Bijel, as macroscopic phase separation of the binary solvent is not a requirement in SeedGel. It also broadens the solvent systems that can be used for SeedGel formation.

While the domain structures maintain the same size at different temperatures in the formed SeedGel, contrast variation USANS experiments reveal the solvent exchange of the organic component of the binary solvent between bicontinuous domains. Combined with previous results, the present work clearly demonstrates that both components of the binary solvent can be exchanged between the two domains of the SeedGel when changing the sample temperature. Using deuterated 3MP can significantly shift the gelation temperature of the SeedGel formation. A close relationship between the correlation lengths of the density fluctuation of binary solvents and the SeedGel formation temperature is observed. It is found that SeedGel is formed when the correlation length in the binary solvent reaches around 2 nm for the charged silica particles used in these studies. This correlation length is likely a function of the particle properties that need to be investigated in future studies.

Acknowledgments

YX and YL thank the financial support from Cooperative Agreement No. 70NANB12H239 and 70NANB10H256 of the National Institute of Standards and Technology (NIST), the U.S. Department of Commerce. AZ acknowledges the funding from the Summer Undergraduate Research Fellowship (SURF) at the NIST. This work benefited from the use of the SasView application, originally developed under NSF Award DMR - 0520547. SasView also contains code developed with funding from the EU Horizon 2020 program under the SINE2020 project Grant No 654000. A portion of this research used resources at the Spallation Neutron Source, a DOE Office of Science User Facility operated by the Oak Ridge National Laboratory. The beam time was allocated to EQ-SANS and USANS on proposal IPTS-27148.1. The statements, findings, conclusions, and recommendations are those of the authors and do not necessarily reflect the view of NIST or the U.S. Department of Commerce. Identification of a commercial product does not imply recommendation or endorsement by NIST, nor does it imply that the product is necessarily the best for the stated purpose.

Competing Interests Statement

Y.X. and Y.L. are inventors on a PCT international patent application related to this work filed by the University of Delaware (no. PCT/US2021/070989 filed [July 27th, 2021]).

References:

1 T. J. Thorson, E. L. Botvinick and A. Mohraz, *ACS Biomater. Sci. Eng.*, 2018, **4**, 587–594.
2 M. F. Haase, K. J. Stebe and D. Lee, *Adv. Mater.*, 2015, **27**, 7065–7071.
3 Y. Cheng, Y. Zheng and Z. Song, *Nanoscale*, 2021, **13**, 4678–4684.
4 G. Di Vitantonio, T. Wang, M. F. Haase, K. J. Stebe and D. Lee, *ACS Nano*, 2019, **13**, 26–31.
5 J. Han, M. J. Lee, K. Lee, Y. J. Lee, S. H. Kwon, J. H. Min, E. Lee, W. Lee, S. W. Lee and B. J. Kim, *Advanced Materials*, 2023, **35**, 2205194.

6 Y. Xi, R. S. Lankone, L.-P. Sung and Y. Liu, *Nat Commun*, 2021, **12**, 910.
7 M. Clausse, J. Peyrelasse, J. Heil, C. Boned and B. Lagourette, *Nature*, 1981, **293**, 636–638.
8 S. Xie, D. J. Meyer, E. Wang, F. S. Bates and T. P. Lodge, *Macromolecules*, 2019, **52**, 9693–9702.
9 S. T. Hyde, *Current Opinion in Solid State and Materials Science*, 1996, **1**, 653–662.
10 E. M. Herzig, K. A. White, A. B. Schofield, W. C. K. Poon and P. S. Clegg, *Nat Mater*, 2007, **6**, 966–971.
11 C. Huang, J. Forth, W. Wang, K. Hong, G. S. Smith, B. A. Helms and T. P. Russell, *Nature Nanotech*, 2017, **12**, 1060–1063.
12 D. Cai and P. S. Clegg, *Chem. Commun.*, 2015, **51**, 16984–16987.
13 J. W. Tavacoli, J. H. J. Thijssen, A. B. Schofield and P. S. Clegg, *Adv. Funct. Mater.*, 2011, **21**, 2020–2027.
14 M. Reeves, A. T. Brown, A. B. Schofield, M. E. Cates and J. H. J. Thijssen, *Phys. Rev. E*, 2015, **92**, 032308.
15 N. Hijnen, D. Cai and P. S. Clegg, *Soft Matter*, 2015, **11**, 4351–4355.
16 L. Bai, J. W. Fruehwirth, X. Cheng and C. W. Macosko, *Soft Matter*, 2015, **11**, 5282–5293.
17 Y. Xi, J. B. Leão, Q. Ye, R. S. Lankone, L.-P. Sung and Y. Liu, *Langmuir*, 2021, **37**, 2170–2178.
18 Y. Xi, F. Zhang, Y. Ma, V. M. Prabhu and Y. Liu, *Nat Commun*, 2022, **13**, 3619.
19 Y. Xi, R. P. Murphy, Q. Zhang, A. Zemborain, S. Narayanan, J. Chae, S. Q. Choi, A. Fluerasu, L. Wiegart and Y. Liu, *Soft Matter*, 2023, **19**, 233–244.
20 J. D. Cox, *J. Chem. Soc.*, 1952, 4606.
21 Schneider, G. M., *Ber. Bunsenges. Phys. Chem.*, DOI:10.1002/bbpc.19720760336.
22 T. Narayanan and A. Kumar, *Physics Reports*, 1994, **249**, 135–218.
23 J. Szydlowski, *Nukleonika*, 1998, **43**, 423–428.
24 R. J. L. Andon and J. D. Cox, *Journal of the Chemical Society (Resumed)*, 1952, 4601.
25 W. T. Heller, M. Cuneo, L. Debeer-Schmitt, C. Do, L. He, L. Heroux, K. Littrell, S. V. Pingali, S. Qian, C. Stanley, V. S. Urban, B. Wu and W. Bras, *J Appl Crystallogr*, 2018, **51**, 242–248.
26 W. T. Heller, J. Hetrick, J. Bilheux, J. M. B. Calvo, W.-R. Chen, L. DeBeer-Schmitt, C. Do, M. Doucet, M. R. Fitzsimmons, W. F. Godoy, G. E. Granroth, S. Hahn, L. He, F. Islam, J. Lin, K. C. Littrell, M. McDonnell, J. McGaha, P. F. Peterson, S. V. Pingali, S. Qian, A. T. Savici, Y. Shang, C. B. Stanley, V. S. Urban, R. E. Whitfield, C. Zhang, W. Zhou, J. J. Billings, M. J. Cuneo, R. M. F. Leal, T. Wang and B. Wu, *SoftwareX*, 2022, **19**, 101101.
27 C. J. Glinka, J. G. Barker, B. Hammouda, S. Krueger, J. J. Moyer and W. J. Orts, *J Appl Crystallogr*, 1998, **31**, 430–445.
28 S. R. Kline, *Journal of Applied Crystallography*, 2006, **39**, 895–900.
29 J. Leys, D. Subramanian, E. Rodezno, B. Hammouda and M. A. Anisimov, *Soft Matter*, 2013, **9**, 9326.
30 M. Teubner and R. Strey, *The Journal of Chemical Physics*, 1987, **87**, 3195–3200.
31 K. -V. Schubert, R. Strey, S. R. Kline and E. W. Kaler, *The Journal of Chemical Physics*, 1994, **101**, 5343–5355.
32 H. Endo, M. Mihailescu, M. Monkenbusch, J. Allgaier, G. Gompper, D. Richter, B. Jakobs, T. Sottmann, R. Strey and I. Grillo, *The Journal of Chemical Physics*, 2001, **115**, 580–600.
33 M. Doucet, J. H. Cho, G. Alina, Z. Attala, J. Bakker, P. Beaucage, W. Bouwman, R. Bourne, P. Butler, I. Cadwallader-Jones, K. Campbell, T. Cooper-Benun, C. Durniak, L. Forster, P.

Gilbert, M. Gonzalez, R. Heenan, A. Jackson, S. King, P. Kienzle, J. Krzywon, B. Maranville, N. Martinez, R. Murphy, T. Nielsen, L. O'Driscoll, W. Potrzebowski, S. Prescott, R. Ferraz Leal, P. Rozyczko, T. Snow, A. Washington, L. Wilkins and C. Wolf, SasView version 5.0.6 Zenodo 2023.

34 Z. Wang, H. Guo, Y. Liu and X. Wang, *The Journal of Chemical Physics*, 2018, **149**, 084905.

35 C. E. Bertrand, P. D. Godfrin and Y. Liu, *The Journal of Chemical Physics*, 2015, **143**, 084704.

The data supporting this article have been included as part of the Supplementary Information.